THERMAL AND STRUCTURAL INVESTIGATION OF $(Sn_{1-x}Ti_x)O_2$ OBTAINED BY THE POLYMERIC PRECURSOR METHOD

M. R. Cassia-Santos[1*], *A. G. Souza*[1], *L. E. B. Soledade*[1], *J. A. Varela*[2] *and E. Longo*[3]

[1]Universidade Federal da Paraíba, DQ, CCEN, LTM, João Pessoa, PB, Brazil
[2]Universidade Paulista, IQ, CMDMC, Araraquara, SP, Brazil
[3]Universidade Federal de São Carlos, DQ, CMDMC/LIEC, São Carlos, SP, Brazil

In the last decade the $(Sn_{1-x}Ti_x)O_2$ system had a great interest. Consequently, due to its great potential application as electronic and ceramic, it has been widely investigated. The aim of the present work was to study the thermal and structural properties of powders $(Sn_{1-x}Ti_x)O_2$, where $0 \leq x \leq 1$, obtained by the polymeric precursor method. TG/DSC and XRD methods were applied to study these systems. The TG curves indicated essentially three-step mass losses related to the dehydration, the degradation of the polymer and to the loss of most of the organic material (pyrolysis). According to the TG data, no mass loss was observed above 600°C. The exotherm DSC peaks correspond to the large mass loss process observed by TG between 300 and 600°C. They are related to the decomposition of the organic matter as well as to the partial crystallization of $(Sn_{1-x}Ti_x)O_2$. It was observed from the XRD results that the lattice parameters (a, c, c/a) and the volume of the unit cell (V) do not vary linearly with the increase of the TiO₂ concentration, presenting a deviation from the Végard law, indicating a phase separation within these samples. This deviation from the linearity, as a function of Sn/Ti concentration ratio can be used to evidence of the phase separation or a strong contraction/shrinkage of the SnO₂ lattice with the addition of TiO₂. It was concluded that the thermal and structural characteristic of the $(Sn_{1-x}Ti_x)O_2$ system depend on the Sn/Ti molar ratio.

Keywords: $(Sn_{1-x}Ti_x)O_2$, SnO₂, structural evolution, TiO₂

Introduction

Both SnO₂ and TiO₂, are *n*-type semiconductors and isomorphous, displaying a tetragonal crystalline structure similar to the rutile structure [1]. TiO₂ differs from SnO₂ in the sintering process, because it does not require the presence of additives to obtain a sintered ceramic piece with high density. One of the main advantage of SnO₂ is that in the absence of additives, since the sintering process is not accompanied by a high densification. Furthermore, its high specific surface area allows it to use as a ceramic sensor [1, 2]. In the literature it is verified that SnO₂, due to its high surface area, has one disadvantage compared to TiO₂, namely the compound exhibits, a high equilibrium pressure of oxygen $(SnO_2(s) \leftrightarrow SnO(g) + 0.5O_2(g))$. This elevated equilibrium pressure of oxygen promotes the decomposition of the substance when it is exposed to a reducing atmosphere for long time period, especially at high temperatures. On the other hand, TiO₂ exhibits a much smaller oxygen equilibrium pressure and, consequently, a higher resistance to reducing atmospheres. Therefore, the conception of a mixed oxide containing the two oxides involving the good sensibility of SnO₂ and the high chemical stability of TiO₂ at high temperatures appears to be a

technological challenge, which has of a growing interest among many authors [3–11].

According to some authors the addition of TiO₂ to the SnO₂ lattice promotes to enhance the densification of SnO₂ and the appearance of non linear electric properties [1, 2, 12] which are typical for the varistor systems [13]. It was mentioned in some papers that these two oxides form solid solution and a large extent [4, 5, 7]. However, this solid solution highly depends on the chemical composition and it is only stable above a critical temperature which is about 1400°C [8–11]. Below this temperature, the system presents an immiscibility range, as a function of its chemical composition. Such a range, in which SnO₂ and TiO₂ are immiscible, is especially interesting, because it is accompanied by the phenomenon of spinodal decomposition. In other words, the solid solution is decomposed into lamellar alternating layers of SnO₂ and TiO₂. As a matter of fact, solid solutions of SnO₂–TiO₂ could be obtained at lower temperatures, even for concentrations in which the phase diagram foresees the occurrence of the spinodal decomposition, since the formation of such a solid solution is kinetically favored [14].

In the present work the thermal and structural properties of the $(Sn_{1-x}Ti_x)O_2$ system synthesized by

* Author for correspondence: csantos@quimica.ufpb.br

the polymeric precursor method, as a function of the heat treatment temperature, were investigated. The formation of a single-phase system and the phase separation, which is typical for the spinodal decomposition were evaluated by XRD.

The polymeric precursor method is based on the pioneer work of Pechini [15] used to synthesize polycation oxide powders. This process is based on metallic citrate polymerization with the use of ethylene glycol. A hydrocarboxylic acid, such as citric acid is employed to chelate cations in aqueous solution. The addition of glycol, such as ethylene glycol, leads to organic ester formation. The polymerization, promoted by heating of the mixture, results a homogeneous resin in which metal ions are uniformly distributed throughout the organic matrix. The powders obtained from this method exhibit a high homogeneity and high superficial area.

Experimental

Tin citrate was separately prepared from $SnCl_2 \cdot 2H_2O$ and the titanium citrates were prepared by the dissolution of titanium(IV) isopropoxide in an aqueous solution of citric acid at 60–70°C. Nitric acid was used to improve the solubility. After obtaining the tin and titanium citrates, ethylene glycol was added to promote the polymerization of the mixed citrates by the polyesterification reaction. The molar ratios between tin and titanium studied were 1:0 (sample Sn); 0.75:0.25 (sample Sn75); 0.50:0.50 (sample Sn50); 0.25:0.75 (sample Sn25); 0:1 (sample Ti). The citric acid/metal molar ratio was fixed at 3:1 and the citric acid/ethylene glycol mass ratio was fixed at 60:40. In this way a clear and transparent resin solution was obtained. After polymerization at temperatures ranging from 70 to 80°C, the resin was treated at 120°C in order to eliminate NO_x and was later heat treated at 300°C for two hours for the pre-treatment of the resin. After then, all materials were calcined for 2 h at several temperatures in order to promote the phase crystallization.

The polymeric precursor, after partial elimination of water and the complete elimination of NO_x (120°C), was characterized by simultaneous thermal analyses, TG/DSC (STA 409, Netzsch, Germany). All these runs were performed in a synthetic air atmosphere (50 cm^3 min^{-1}), using a 10 K min^{-1} heating rate from room temperature up to 800°C. The crystallization process was observed by means of a grazing incidence X-ray diffraction, carried out in a Rigaku model D Max 2500PC, in the Bragg θ-2θ geometry. This diffractometer was equipped with a graphite monochromator and a CuK$_\alpha$ radiation (λ=1.5418 Å), operating with 40 kV voltage and 150 mA of emission current. Data were obtained with a step times of 8.0 s

and a step size of 0.020° (2θ) between 20–110°. The lattice parameters were refined by the 'Rede 93' software, which is based on the least square method, using powdered metallic silicon (at the mass proportion of 30%) as an internal standard.

Results and discussion

Thermogravimetric analysis

The TG curves allow gathering information with regard to the thermal stability of the sample, the intermediate and final products, as well as the composition. Figures 1 and 2 present the results of the thermal analyses (TG/DSC) of the different samples studied (Sn, Sn75, Sn50, Sn25 and Ti).

TG curves are shown in Fig. 1a, indicate the mass losses all along in the investigated temperature range. Essentially, three mass loss steps could be distinguished:
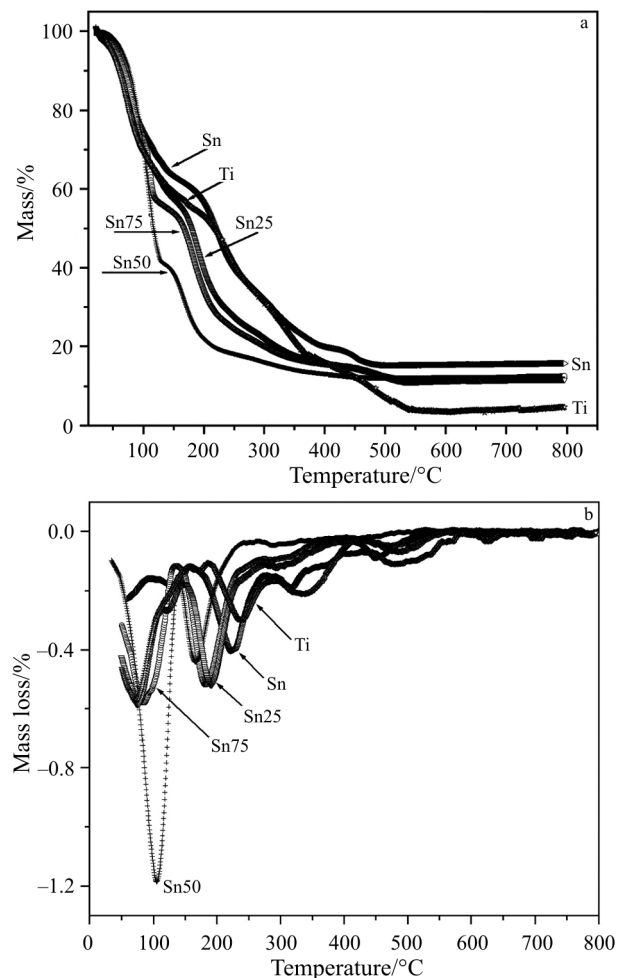

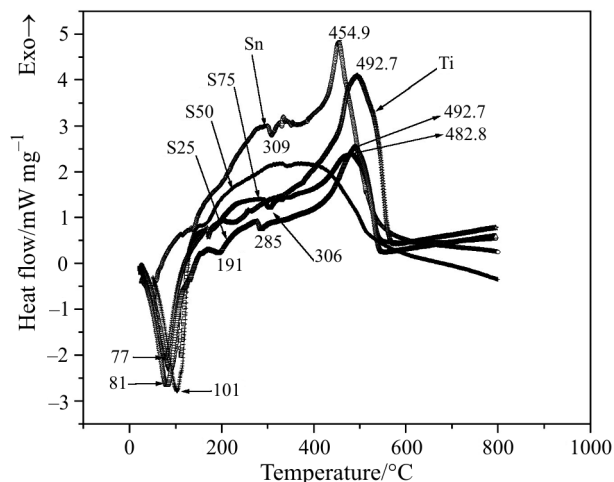**Fig. 1** a – TG and b – DTG curves of Sn, Sn75, Sn50, Sn25 and Ti samples

Fig. 2 DSC curves of Sn, Sn75, Sn50, Sn25 and Ti samples

1 Up to approximately 200°C water elimination takes place and begins the elimination of the volatile organic solvent;

2 From 200 up to 380–400°C the polymer degradation can be seen, with the formation of CO_2 and H_2O, loosing a remarkable part of the organic material;

3 Above 400°C the remainder of the organic material leaves with the elimination of the carboxyls and of the residual carbon, with different mass loss rates.

Above 600°C, no mass loss was observed. It indicates that the organic compounds were totally eliminated and the complete crystallization of the $(Sn_{1-x}Ti_x)O_2$ took place.

In the DSC curves of the different samples (Fig. 2), endotherm peaks appeared between 75–175°C. They related to the evaporation of water and to the beginning of the evolution of the organic matter, followed by consec-
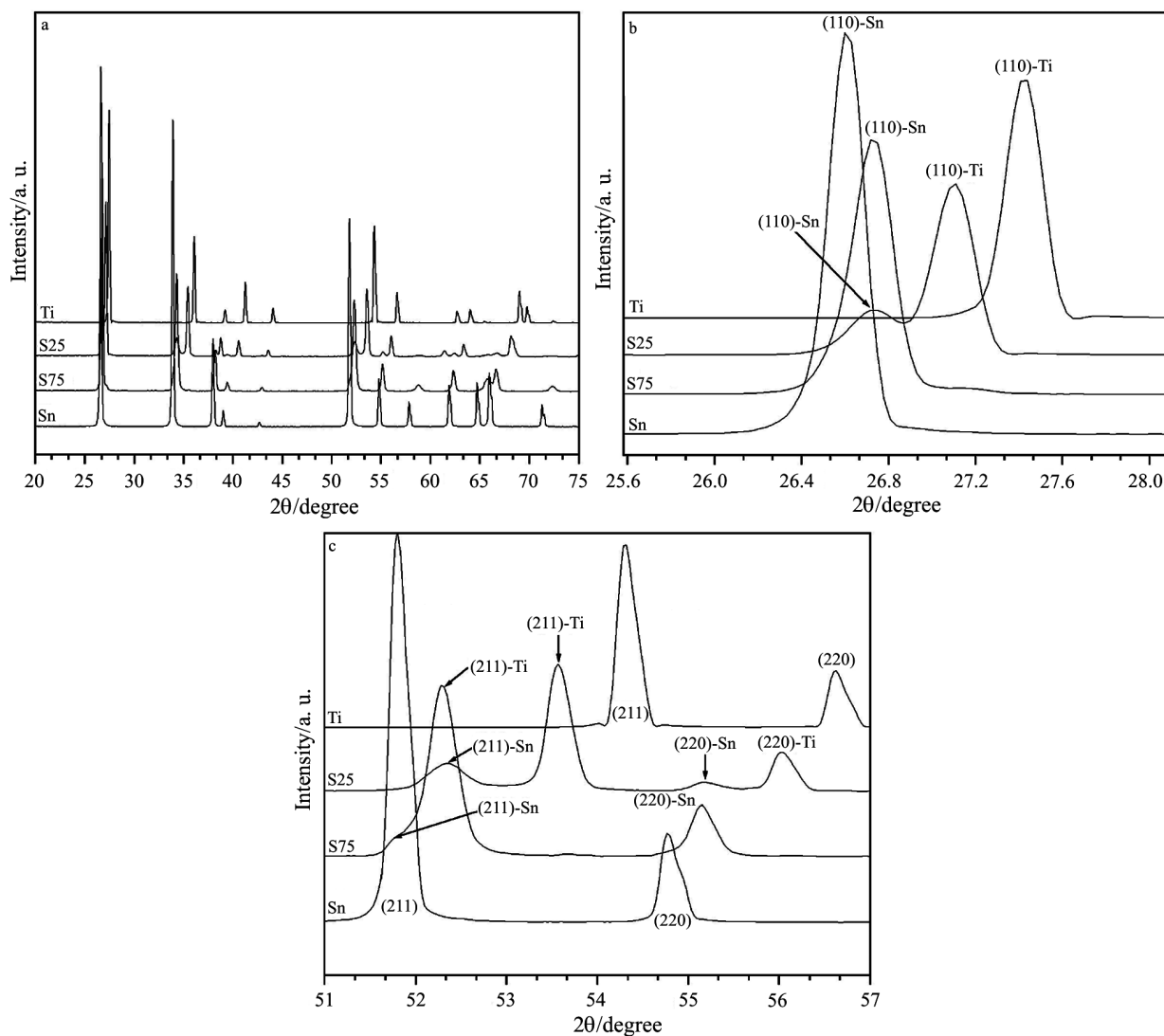

Fig. 3 X-ray patterns indicating the phase evolution observed for the powders of the $(Sn_{1-x}Ti_x)O_2$ binary system obtained by the polymeric precursor method, and treated at 1200°C for 2 h. X-ray patterns in a – all along the investigated range, enlargement of the b – 25°<2θ<28° (Sn=SnO₂; Ti=TiO₂) and c – 51°<2θ<57° ranges

utive exothermic reactions leading to the complete oxidative decomposition of the polymer. In the range of 380–550°C, well defined exothermic peaks can be observed which might attributed to the elimination of the residual organic substance (carboxyls and residual carbon).

Phase identification by XRD

Aiming to identify the formation of either a single phase system or a system presenting the phase separation typical of spinodal decomposition, the evolution of the crystalline phases of the $(Sn_{1-x}Ti_x)O_2$ system was evaluated by XRD. From the XRD results the values of the lattice parameters, a and c, were obtained and using them the volume of the unit cell (V) and the tetragonality factor (c/a), could be calculated.

According to Fig. 3a the appearance of the diffraction peaks (indicated by arrows) in Sn25 are different from the SnO_2 or TiO_2. In Figs 3b and c, the X-ray

diffraction patterns are enlarged in order to show more clearly the 2θ ranges where these diffraction peaks are appeared. In the 25°<2θ<28° degree interval for the Sn25 sample the appearance of two peaks was observed. The first one is at 2θ≅26.6° and the second is at 2θ≅27.2°. These peaks can be attributed to the (110) SnO_2 and (110) TiO_2 diffractions, as it was observed by Naidu *et al.* [15] and Hirata *et al.* [3].

According to Fig. 3c, Sn25 and Sn75 samples exhibit two diffraction peaks within this interval. For Sn75 the first one is a small band at 2θ≅51.8° [related to the (211) plane of SnO_2], and the second is a more intense peak at 2θ≅52.6° [related to the (211) plane of TiO_2]. As for Sn25, there are peaks at 2θ≅52.3° and at 2θ≅53.7°. Two further small diffraction bands at 2θ≅55° and 2θ≅56° could be observed. They are possibly due to the (220) diffractions for the SnO_2-rich and for the TiO_2-rich systems. These results evidence that the powders synthesized by the polymeric precursor method and thermally treated at 1200°C present spinodal decomposition.
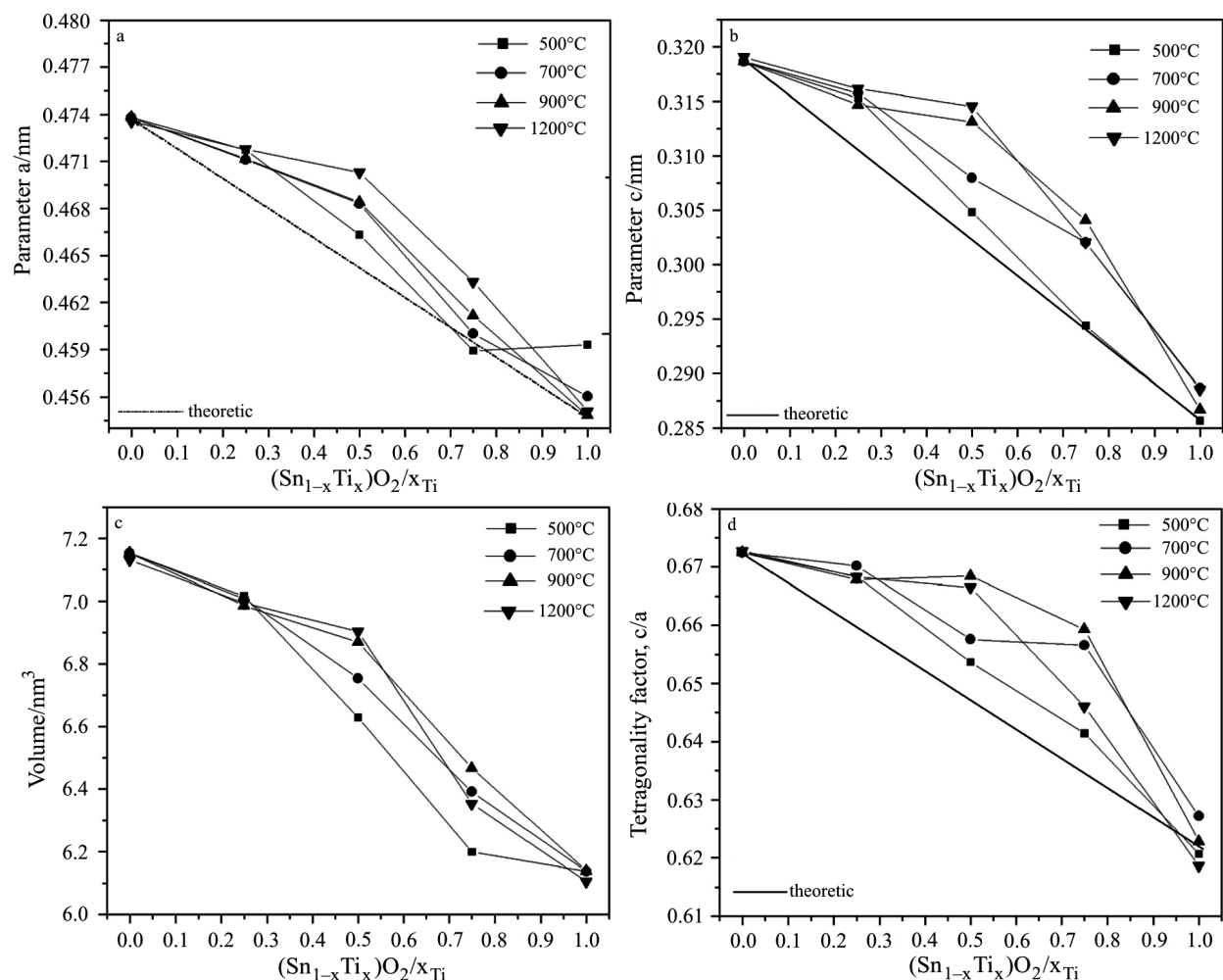

Fig. 4 a – Lattice parameter a, b – lattice parameter c, c – volume of the unit cell and d – tetragonality factor c/a, of the $(Sn_{1-x}Ti_x)O_2$ samples obtained by the polymeric precursor method, treated at different temperatures

From the XRD measurements the characteristic lattice parameters of the binary oxide systems were possible to evaluate. As it has been previously mentioned, both SnO_2 and TiO_2 oxide have the same crystalline symmetry, displaying different lattice parameters, however they are close together. Therefore, one extremely important step, upon appraising the structural properties of the binary oxide system is the evaluation of the possible variations occurred in the lattice parameters of SnO_2 after the addition of TiO_2.

In Fig. 4 the calculated values of the lattice parameters, c and a, are plotted as a function of x for $(Sn_{1-x}Ti_x)O_2$. The axial ratio c/a and the unit-cell volume $V=a^2c$ are also presented. A comparison of these results with experimental data reported by Hirata *et al*. [3] shows a good agreement. It is evident that the lattice parameters and cell volume of the solid solutions decrease with x indicating the lattice contraction. However, the magnitude of the corresponding structural parameters, a and c, do not vary linearly with x; therefore, some deviation from Vegard's law was found. This is the expected result, since this is associated to the replacement of some Sn^{4+} ions by Ti^{4+} ions, as it was observed by other authors [3, 6, 7, 16–19]. This substitution can promote a distortion of the SnO_2 lattice towards reducing the lattice parameter values (a and c) and consequently reducing the volume of the unit cell (V) and the tetragonality factor (c/a), since a smaller ion replaces a bigger one in the lattice. Hirata *et al*. [3] and Park *et al*. [11] also reported positive deviations from the Vegard's law in the $Sn_xTi_{1-x}O_2$ system. The lattice parameters are bigger than those obtained just from a linear interpolation from the endpoint binary oxides TiO_2 and SnO_2. Thus, our results indicate that the deviation from the Vegard's law in the $Sn_xTi_{1-x}O_2$ solid solution is not a consequence of the spinodal decomposition. However, the indicated deviation is frequently accompanied by phase separation caused by spinodal decomposition.

Such phase separation occurred when Ti/(Sn+Ti) ratio was between 40 and 60% in the lattice [3, 6, 14, 18, 19]. The deviation from the Vegard's law is related to the big repulsion that takes place in the crystal lattice, for instance of SnO_2, due to the addition of TiO_2. The formation of spinodal decomposition promotes modification in the crystal lattice causing a positive deviation from the linearity.

The experimentally determined c/a ratio for the Sn50 sample is 0.654. The calculated value using the JCPDS records is 0.673 for SnO_2 and 0.643 for TiO_2. The c/a value for the Sn50 system is lower than the theoretical one for the SnO_2 lattice, evidencing the lattice contraction upon the replacement of Sn^{4+} by Ti^{4+}, since Ti^{4+} has a slightly smaller ion radius than the Sn^{4+} has.

Conclusions

Concluding from the TG results, the mass losses basically take place in three different steps, ascribed to the release of water and to the degradation of the polymers, decomposing to CO_2 and H_2O and to the loss of a major part of the organic material. According to the TG experiments no further mass loss was observed over 600°C. By the evaluation of the DSC curves, the onset temperature of the crystallization of the precursor powders are approximately in the same temperature range. From the TG and XRD results the thermal and structural evolution of the $(Sn,Ti)O_2$ system, as a function of the thermal treatment temperature could be observed. The deviation from the Vegard's law confirms the phase separation, which is typical from the spinodal decomposition, and can be identified for the different compositions of this system. The variation of the SnO_2 lattice parameter values upon the addition of TiO_2 illustrates the contraction of the lattice as a function of the replacement of Sn^{4+} by Ti^{4+}. All the studied properties of the $(Sn_{1-x}Ti_x)O_2$ system were shown to depend on the Sn/Ti molar ratio.

Acknowledgements

References

1 Z. M. Jarzebbski and J. P. Marton, J. Electrochem. Soc., 129 (1976) 299c.
2 J. A. Cerri, E. R. Leite, D. Gouvea, E. Longo and J. A. Varela, J. Am. Ceram. Soc., 79 (1996) 799.
3 T. Hirata, K. Ishioka, M. Kitajima and E. H. Doi, Phys. Rev. B, 53 (1996) 8442.
4 M. Radecka, K. Zakrzewska and E. R. Mieczyslaw, Sens. Actuators B, 47 (1998) 194.
5 M. Radecka, P. Pasierb, K. Zakrzewska and M. Rekas, Solid State Ionics, 119 (1999) 43.
6 J. Lin, J. C. Yu, D. Lo and S. K. Lam, J. Catal., 183 (1999) 368.
7 F. Edelman, H. Hahn, S. Seifried, C. Alof, H. Hoche, V. Mikhelashvili and G. Eisenstein, Mat. Sci. Eng. B-Solid, 69–70 (2000) 386.
8 V. S. Stubican and A. H. Schultz, J. Am. Ceram. Soc., 51 (1968) 290.
9 V. S. Stubican and A. H. Schultz, J. Am. Ceram. Soc., 53 (1970) 211.
10 D. Garcia and F. Speidel, J. Am. Ceram. Soc., 55 (1972) 322.
11 M. Park, T. E. Mitchell and A. H. Heuer, J. Am. Ceram. Soc., 58 (1975) 43.
12 P. R. Bueno, M. R. S. Bosso, C. O. Paiva-Santos, E. Longo and L. O. S. Bulhões, J. Eur. Ceram. Soc., 23 (2003) 887.

13 M. R. Cassia-Santos, P. R. Bueno, L. G. P. Simões, J. W. Gomes, E. Longo and J. A. Varela, J. Am. Ceram. Soc., 85 (2002) 282.

14 S. K. Kulshreshtha, R. Sasikala and V. Sudarsan, J. Mater. Chem., 11 (2001) 930.

15 M. P. Pechini, U.S. Patent 3,330,697 (1967).

16 H. P. Naidu and A. V. Virkar, J. Am. Ceram. Soc., 81 (1998) 2176.

17 V. Dusastre and D. E. Williams, J. Mater. Chem., 9 (1999) 445.

18 L. B. Kong, J. Ma and H. Huang, J. Alloys Compd., 336 (2002) 315.

19 W. Y. Chung, D. Lee and B. K. Sohn, Thin Solid Films, 221 (1992) 304.